Hybrid Baseline Localization for Portable AUV Navigation

Bryce Gill[1], David Schipf[1], Ryan Borth[1], John Canning[1], Eric Wolbrecht[1], Michael Anderson[1], Dean Edwards[2]

[1]Department of Mechanical Engineering, University of Idaho, Moscow, Idaho

[2]Department of Chemical Engineering, University of Idaho, Moscow, Idaho

***Abstract*— In this paper we present experimental and simulated results for an improvement upon the moving short baseline (MSBL) method of navigation for a fleet of autonomous underwater vehicles (AUVs). With the goal of maintaining system simplicity and portability, the hybrid baseline (HBL) approach utilizes one or both of the objective ship-mounted MSBL transponders in conjunction with a single off-path drifting buoy-mounted transponder intended to resolve problems observed in previous MSBL navigational work. The states of the ship and buoy are estimated using extended Kalman filters (EKFs) that are updated with state broadcasts from each source. Because the system uses a synchronous communication cycle, the AUVs are also able to calculate ranges with each broadcast; with the addition of onboard sensor data, the AUVs are able to use these ranges to estimate their own state using a third EKF. Simulation and field test results indicate that with respect to previous MSBL results, the perpendicular-to-path range data from the buoy allows the EKF to more quickly reduce the initialization error in the AUV position and maintain a lower overall position error.**

***Keywords*—AUV navigation; moving baseline; acoustic ranging.**

I. Introduction

In the modern era, sea mines constitute one of the largest threats to U.S. Naval vessels [1]. Sea mines are frequently triggered upon detection of the magnetic disturbance caused by a passing ship. Currently techniques exist for minimizing a ship's magnetic field, the effectiveness of which depends upon the accuracy of available data regarding the ship's field. This magnetic signature data is traditionally acquired either in dry-dock or at a static testing range. Because the magnetic field generated by a ship depends partly on environmental factors, such as the Earth's local magnetic field and the local salinity of sea water, the quality of this data can be improved by taking measurements in situ as conditions and location change. An up-to-date magnetic signature assessment of this kind may significantly improve the potential effectiveness of any field cancellation techniques employed.

With this goal of portability in mind, the University of Idaho (UI) is currently developing a fleet of autonomous underwater vehicles (AUVs), seen in Fig. 1, capable of measuring the magnetic signature of an objective vessel. With real-time GPS data unavailable during normal operation, these AUVs navigate with a combination of dead-reckoning (using onboard sensor data) and acoustic ranging from external sources. Because the quality of the measured magnetic field data depends directly on the accuracy of the navigation during collection, it is critical that the AUVs trajectory is accurate in-mission and that its localization is accurate in post-processing.

Fig. 1. The University of Idaho fleet of AUVs.

In order to determine an appropriate navigation method that meets the portability and accuracy requirements, it is helpful to understand the shortcomings of previous navigation work – which has typically focused on three primary methods [2]: long baseline (LBL), short baseline (SBL), and ultra-short baseline (USBL). Additional methods include simultaneous localization and mapping (SLAM), use of one or more communication and navigation aid(s), and moving baseline approaches (MBL).

Traditional LBL navigation utilizes an array of fixed transponders arranged with large separation relative to the distance between the AUV and the transponder array, as in [3-4] LBL transponder geometry is often defined such that the AUV operates within the bounds of the transponder array. While this method demonstrates a suitable degree of accuracy, the physical requirements of the transponder array prevent portable operation.

SBL navigation [5] is generally similar to LBL except that the transponders are located closer to one another than they are to the AUV, with AUV operation typically taking place outside of the transponder array. This change in configuration comes with a reduction in the accuracy of AUV localization through acoustic ranging. SBL navigation is insufficient in this case both for accuracy and portability reasons.

USBL navigation, in which ranging transponders are located very close together, is becoming more widely used as technology and methods improve, as demonstrated in [6].

978-0-933957-40-4 ©2013 MTS

Although precision methods have been developed using USBL navigation, the AUV localization is often done external to the AUV. Because USBL navigation operates on such small array scales it has the additional difficulty of highly intensive measurement and calibration requirements.

SLAM navigation [7] and single-source navigation [8] are limited in suitability similarly to LBL and SBL navigation when considering the issues of portability and accuracy. Both require either *a priori* knowledge of the local geometry or a set of fixed reference points. In either case, operation is subject to conditions which are impossible or impractical for portable operation.

MBL navigation provides a portable solution, and for the purpose of discussion in this paper can be divided into two different areas: moving short baseline (MSBL) navigation as seen in [9-11], in which the ranging transponders are separated by small distances relative to their distance from the AUV; and moving long baseline (MLBL) navigation as in [12-14], in which the ranging transponders remain far apart.

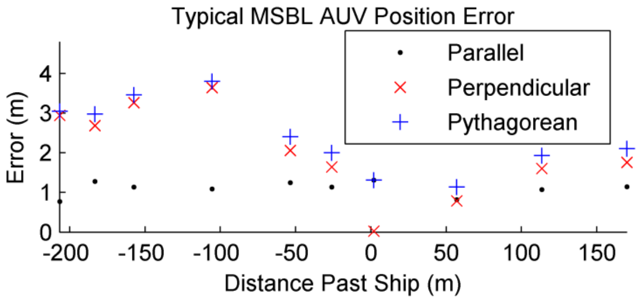

Fig. 2. Accuracy of the AUV EKF during a typical MSBL mission. The initialization error remains until the AUV approaches the objective ship and is only partially corrected by the end of the mission. The AUV and ship cross in this run at ~120 s (when distance past ship equals zero).

MSBL navigation is the simpler of these two cases, providing the AUVs with all necessary ranging data while only requiring that a single external object be tracked. In this navigation method, two transponders are mounted on the objective ship and use a synchronous communication cycle to simultaneously broadcast ship state information and provide the AUVs with range data. Experimental results for MSBL navigation at UI demonstrate a persistent error in the AUV position estimate that is dependent upon the accuracy of initialization. This error remains until the AUVs near the objective ship, at which time localization accuracy moderately improves. This occurs because when the AUV is far from the ship, it receives very little range data perpendicular to its path; as it approaches the ship its angle to the transponders increases and it is able to make lateral corrections. Fig. 2 illustrates the difficulty of MSBL navigation clearly: although the AUV receives strong parallel-to-path range data from the objective ship (indicated by consistently low parallel-to-path error), it receives little perpendicular-to-path range data until it is within close proximity to the objective ship. While MSBL navigation has proven a stable method for AUV localization and demonstrates a reasonable degree of accuracy, further reduction of navigational error is desired.

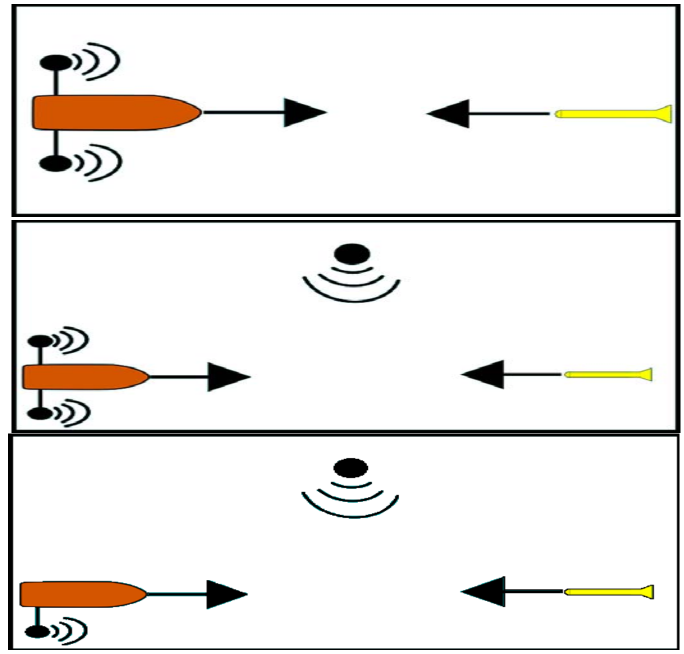

Fig. 3. Mission geometry for standard MSBL (top) and HBL missions. An MSBL mission utilizes a pair of transponders mounted on either side of the target ship for ranging. HBL includes an additional floating transponder located off the waypoint path, using either both (middle) or only one (bottom) of the MSBL ship-mounted transponders.

MLBL navigation expands upon the complexity of MSBL by utilizing communication and navigation aide (CNA) vehicles; in the case of both simulated and experimental results, these consisted of controllable surface vehicles that provide the AUVs with ranging data. The advantage of this system is that the addition of CNAs was able to successfully address the issues seen in MSBL operation (especially in [15], in which the CNA operation was combined with the above-described MSBL system). The CNA vehicles could be maneuvered to optimize the amount of perpendicular-to-path ranging data available to the AUV and reduce the AUVs' lateral position error before they reached the objective ship. This additional information came, however, at the cost of increased system complexity. In addition to tracking and estimating the position of the objective ship, the AUV also was required to track the positions of one or more CNA vessels – each of which had to have its own control authority and synchronize its mission operation and position with that of the AUV-ship system.

In response to the shortcomings of the above-discussed navigational methods, this paper proposes a combination of methods with the goal of taking advantage of the most useful aspects of portable systems while improving upon MSBL accuracy without a significant increase in system cost and complexity. The resulting hybrid baseline (HBL) navigation utilizes one or both ship-mounted MSBL transponders in addition to a single, drifting buoy-mounted transponder located off the AUV waypoint path (see Fig. 3). The AUVs will be required to track and estimate the position of the buoy, but the buoy itself remains uncontrolled and subject to drift.

II. Methods

A. State Estimation

Following previous work at UI [9], the extended Kalman filter (EKF) as described in [16] is used onboard each AUV to estimate its own state as well as that of the objective ship and floating buoy. The EKF combines onboard sensor data, acoustic ranges, and a kinematic propagation model. Each of the EKFs described below utilize a propagation model $\boldsymbol{f}_{k-1}$ that describes the current state $\boldsymbol{X}_k$ in terms of the previous state $\boldsymbol{X}_{k-1}$ and an update model $\boldsymbol{h}_k$ that relates the measurements $\boldsymbol{z}_k$ to the current state. These propagation and update models are given mathematically by

$$\boldsymbol{X}_k = \boldsymbol{f}_{k-1}(\boldsymbol{X}_{k-1}, \boldsymbol{u}_{k-1}, \boldsymbol{w}_{k-1}) \tag{1}$$

and

$$\boldsymbol{z}_k = \boldsymbol{h}_k(\boldsymbol{X}_k, \boldsymbol{v}_k), \tag{2}$$

respectively. The $\boldsymbol{u}$, $\boldsymbol{w}$, and $\boldsymbol{v}$ terms are the driving function inputs, process noise, and measurement noise, respectively. In the equations presented below, quantities will be given a superscript of "A" to indicate the AUV EKF, an "S" to indicate ship EKF, and a "B" to indicate buoy EKF.

1) AUV State Estimation

In order to measure parameters of its own state, each AUV is equipped with a suite of onboard sensors including a depth sensor, magnetic compass, accelerometer and inertial measurement unit (IMU). Further details of the onboard sensors are discussed in the *Field Testing* section; it is sufficient here to note that the high accuracy of the pressure based depth sensor allows AUV state estimation to be limited to the horizontal plane.

Thus, the state vector, $\boldsymbol{X}^A$, for the AUV EKF can be formulated as

$$\boldsymbol{X}^A = [E^A \quad N^A \quad S^A \quad \psi^A \quad b^A]^T, \tag{3}$$

where E^A and N^A are the AUV's local east and north position, respectively; S^A is its speed (determined by power output to the propeller); ψ^A is its heading; and b^A is the heading bias. The bias term is included to correct for magnetic disturbances (such as the passing objective ship) or calibration errors [17].

The propagation model for the AUV EKF was determined using a kinematic model for the AUV's in-plane motion. Given the accuracy of the onboard depth measurement, it can be assumed that the depth is well-regulated and the vertical component of velocity negligible. The model takes the standard form described in (1). The process noise (w_E^A, w_N^A, w_S^A, w_ψ^A, and w_b^A) is modeled as additive and the driving functions consist solely of the angular acceleration about the vertical axis (rate of heading change) as measured by the IMU, defined as $\dot{\psi}_m^A$. The propagation model is given by

$$\boldsymbol{f}_{k-1}^A = \begin{bmatrix} E_{k-1}^A + \Delta t\, S_{k-1}^A \sin \psi_{k-1}^A + w_E^A \\ N_{k-1}^A + \Delta t\, S_{k-1}^A \cos \psi_{k-1}^A + w_N^A \\ S_{k-1}^A + w_S^A \\ \psi_{k-1}^A + \Delta t\, \dot{\psi}_m^A + w_\psi^A \\ b_{k-1}^A + w_b^A \end{bmatrix}_{k-1}. \tag{4}$$

Through use of the EKF, the onboard dead-reckoning capability is augmented using acoustic ranges to extra-vehicle sources. In the HBL case, range sources include one or two objective ship-mounted transponders as well as the floating buoy-mounted transponder. The measurement vector for the AUV EKF is

$$\boldsymbol{z}^A = [r_1 \quad r_2 \quad r_3 \quad S_m^A \quad \psi_m^A]^T, \tag{5}$$

where r_{1-3} are ranges from the port and starboard ship-mounded transponders and the floating transponder respectively, S_m^A is the measured speed (approximated using power input to the propeller), and ψ_m^A is the heading measured by the onboard compass. Continuing to follow the EKF model laid out in [16], the measurement model takes the form of (2) with

$$\boldsymbol{h}_k^A = \begin{bmatrix} \sqrt{(E_k^A - E^{T_1})^2 + (N_k^A - N^{T_1})^2} + \frac{r_1}{c} v_{tof} + c v_c \\ \sqrt{(E_k^A - E^{T_2})^2 + (N_k^A - N^{T_2})^2} + \frac{r_2}{c} v_{tof} + c v_c \\ \sqrt{(E_k^A - E^{T_3})^2 + (N_k^A - N^{T_3})^2} + \frac{r_3}{c} v_{tof} + c v_c \\ S_k^A + v_S^A \\ \psi_k^A + b_k^A + v_\psi^A \end{bmatrix}. \tag{6}$$

$E^{T_{1-3}}$ and $N^{T_{1-3}}$ are the east and north positions of the transponders from which ranges r_{1-3} in (5) are calculated, and c is the speed of sound in water. Because the ranges are compound measurements determined using measurements of the speed of sound and range time of flight, the measurement model utilizes the terms v_c and v_{tof} to account for noise present in those measurements. The measured speed and heading are modeled with additive noise terms v_S^A and v_ψ^A respectively.

2) Objective Ship and Buoy State Estimation

Because the ship and buoy are both external to the AUVs and capable of broadcasting information about their own current state during a mission, the two EKFs used to track them are identical in form. For simplicity the following descriptions are done in terms of the ship; however, everything in this section applies equally to the floating buoy.

In order to calculate the absolute position of the ship-mounted transponders, the AUVs need access to the ship's current position and heading; in order to complete a kinematic model of the ship, the AUVs further need access to the ship's speed. The ship EKF state vector is therefore described by

$$\boldsymbol{X}^S = [E^S \quad N^S \quad S^S \quad \psi^S]^T, \tag{7}$$

with individual terms defined in the same manner as the corresponding AUV EKF terms (excepting the compass bias term, which is absent in the ship EKF). The dynamic propagation model is similarly defined as

$$\boldsymbol{f}_{k-1}^{S} = \begin{bmatrix} E^S + \Delta t\, S^S \sin\psi^S + w_{E^S} \\ N^S + \Delta t\, S^S \cos\psi^S + w_{N^S} \\ S^S + w_{S^S} \\ \psi^S + \Delta t\, \dot{\psi}^S + w_{\psi^S} \end{bmatrix}_{k-1}, \tag{8}$$

again with terms defined as before.

The ship EKF is updated using individually broadcast measurements of its state vector values; this gives a measurement vector of

$$\boldsymbol{z}^S = [E_m^S \quad N_m^S \quad S_m^S \quad \psi_m^S]^T. \tag{9}$$

Because the ship measurement vector matches directly with the ship state vector, the EKF update model simply consists of including the measurement noise additively:

$$\boldsymbol{h}_k^S = \boldsymbol{X}_k^S + \boldsymbol{w}^S. \tag{10}$$

It is worth noting here one major difference between the operation of the ship and buoy EKFs. In general, the ship's motion is dynamic enough that it requires update measurements for each of its states to converge. The buoy, however, is uncontrolled and subject to surface drift which can be modeled as slow and approximately linear over short timescales. Therefore, although the buoy EKF is capable of accepting measurements for each of its states, in the interest of system simplicity it will be implemented using only measurements of its east and north position. Because the EKF kinematic model utilizes the buoy's speed and heading states to estimate its north and east states, updating the east and north states is sufficient to determine the entire state vector.

B. Communication

1) WHOI modem

In order to facilitate the broadcast and reception of acoustic messages, the UI AUV fleet and support vehicles have been outfitted with a modem designed by the Woods Hole Oceanographic Institute (WHOI). The WHOI modem is capable of handling a synchronous broadcast cycle, the timing of which is managed by a pulse-per-second signal from GPS [18]. This allows the AUVs to use one-way travel-time (OWTT) messaging and range calculations based on the time-of-flight from the message origin.

The WHOI modem has the further capability of broadcast and receipt of either a 13-bit message or a 32-byte message; based on past experience at UI and as reported in [9], it is good practice to allow a two-second interval for each 13-bit message and a six-second interval for each 32-byte message. Despite the greater information bandwidth provided by 32-byte messages, it has been determined [9] that a communication cycle based on 13-bit messages provides sufficient data to estimate necessary states of non-AUV fleet members while additionally providing a greater number of range measurements for use in AUV state estimation.

As discussed in the *Simulation* and *Field Testing* sections, the 13-bit message size creates an important limitation on the measurements available to the AUV. In order to maximize the effectiveness of communications and the robustness of the system, the 13-bit messages are broken into a 5-bit header and an 8-bit payload. The header serves to identify the type of message being broadcast (e.g. "East" or "Speed") and the source of the message, while the payload contains the measured quantity, indexed to pre-defined quantization bounds that are defined separately for each type of measurement relayed via 13-bit acoustic messages. Details of the quantization bounds are discussed below.

2) Communication Cycle

In practice during previous AUV testing at UI using the WHOI modem, it has been determined that a 13-bit message during a synchronous broadcast cycle requires a minimum two-second window for successful transmission and receipt. The communication cycle for HBL missions therefore consists of a repeating series of two-second intervals, each of which contains a single 13-bit message.

For fleet operations, a single cycle slot is given to a progress broadcast by the AUV fleet leader. This information is leveraged by the rest of the fleet to determine the leader's approximate position along the waypoint path, allowing each fleet member to adjust its speed and swim in its designated formation position. An additional two-second silent interval is added to the end of each cycle for communication maintenance processes.

In previous work at UI [9-11] it has been shown that a MSBL mission configuration is successful with a 12-second cycle consisting of one ship broadcast for each of the ship EKF states, one AUV fleet leader broadcast, and the two-second silence buffer. This provides the AUVs with a single update for each ship state during each cycle (for a mission-average rate of 0.083 Hz for each ship EKF measurement) and four range measurements for the AUV EKF (0.33 Hz).

In determining the structure of the HBL broadcast cycle, it is important to consider the number and density of measurements required to maintain accurate buoy and ship EKF states. It is worth noting also that the range measurements taken from each source will have different effects on the AUV EKF. As seen in MSBL tests at UI, the majority of objective-ship-sourced ranges affect primarily the AUV EKF east state because the vector between the ship transponders and the AUV is nearly parallel to the waypoint path (which is either east to west or vice versa). Ranges from the floating buoy are designed to affect primarily the AUV EKF north state.

To help determine the relative importance of each of these factors on overall AUV performance, two different communication cycles were considered (shown in Table 1). The first cycle is based on the previously-used MSBL cycle described above, augmenting it with two additional cycle slots to accommodate the buoy's east and north position broadcasts. The second cycle was extended to 20 seconds by adding an additional east position broadcast from the ship and an additional north position broadcast from the buoy. The 20-second cycle was determined in part based on practical advantages in testing (the cycle is evenly divisible into one minute) and in part based on an assertion (verified in simulation) that AUV performance would be more improved by additional east and north broadcasts from the ship and buoy respectively than by other additional broadcasts.

Table 1 gives a side-by-side comparison of the broadcast positions for each communication cycle considered for HBL navigation as well as those for the MSBL cycle being used as a baseline point of comparison. Table 2 compares the mission-average data rate for the entire set of measurements used to update the system's various EKFs. These provide a good overview of the HBL communication cycle and a background against which the relative importance of each measurement and broadcast can be evaluated.

TABLE 1. COMMUNICATION CYCLES – BROADCAST TIMING

Time (s)	Cycle Name		
	MSBL	**HBL Short**	**HBL Long**
0	Ship East	Ship East	Ship East
2	Ship North	Ship North	Ship North
4	Ship Speed	Buoy East	Buoy North
6	Ship Heading	Ship Speed	Ship Speed
8	Fleet Leader	Ship Heading	Ship Heading
10	Silent	Buoy North	Buoy East
12	---	Fleet Leader	Fleet Leader
14	---	Silent	Ship East
16	---	---	Buoy North
18	---	---	Silent

TABLE 2. COMMUNICATION CYCLES – DATA RATES

Broadcasted Value	Cycle		
	MSBL	**HBL Short**	**HBL Long**
Ship East	0.083 (Hz)	0.063 (Hz)	0.100 (Hz)
Ship North	0.083	0.063	0.050
Ship Speed	0.083	0.063	0.050
Ship Heading	0.083	0.063	0.050
Buoy East	---	0.063	0.050
Buoy North	---	0.063	0.100
Ship Range	0.333	0.250	0.250
Buoy Range	---	0.125	0.150

C. Simulation

For ease of optimization and low-cost analysis of alternative configurations, a simulation was developed using MATLAB® software. The goal for simulation was to accurately model each of: mission scale and objectives; vehicle dynamics and control; communication and measurement; and noise and error. The parameters described below in each of these areas are designed to model as closely as possible the conditions seen in actual field testing.

1) Simulation Parameters

The simulated missions take place in a measurement zone with dimensions of 400 m (east) by 150 m (north), with an east-west waypoint path 200 m long centrally located in the zone. The waypoint path is oriented in an east-west direction, with the AUV traveling east and the ship traveling west. The measurement zone is defined to provide bounds for WHOI message quantization of horizontal coordinates. The AUV and objective ship begin at opposite ends of the waypoint path and travel towards each other at approximately 0.85 m/s and 1.3 m/s, respectively. Both vehicles' headings are controlled as in [19] using the MOOS waypoint-following algorithm. The buoy's position changes on a per-run basis, but is always located in a region to the north of the waypoint path, bounded by the path's ends and the north bound of the measurement zone. The simulated mission terminates when the ship has reached its final waypoint.

At this scale, the 8-bit payloads allow for east and north position broadcast resolutions of 1.57 m and 0.59 m, respectively. The speed and heading broadcasts are likewise quantized, with ranges of 0-4 m/s and 0-2π radians respectively; Table 3 gives a comparison of all quantization ranges and resolutions used.

TABLE 3. QUANTIZATION BOUNDS AND RESOLUTIONS

Measurement	**Range**	**Resolution**
East Position	0 – 150 m	1.57 m
North Position	0 – 400 m	0.59
Speed	0 – 4 m/s	0.016 m/s
Heading	0 – 2π rad	0.025 rad

Noise modeled in this simulation can be seen in the true and EKF state initializations as well as in the measurements. Vehicle starting point was normally distributed about the prescribed starting point with a standard deviation of 5 m to model surface drift conditions prior to mission start. Vehicle speed was similarly initialized with a standard deviation of 0.1 m/s, while heading was randomly distributed from 0 to 2π radians. The true initial conditions were then measured with a Gaussian noise model to provide the initial EKF states. East and North EKF states were initialized with a standard deviation of 4 m to simulate the accuracy of GPS, and speed and heading with standard deviations of 0.05 m/s and 0.1 rad respectively to model the accuracy of the AUV's onboard sensors. The bias state for the AUV EKF was initialized at zero.

The ship and buoy true positions and EKF East and North states were initialized in the same manner and with the same Gaussian noise model. Ship true and EKF speed and heading were initialized following the AUV initialization model, while buoy speed and heading were designed to model a variety of surface drift conditions. Buoy heading was random about a 2π radian interval and speed was normally distributed about zero with a standard deviation of 0.1 m/s. Because the buoy had no control authority, its heading control during simulation was similarly designed to model drift conditions. Due to the short run duration (typically ~200 s) it can be reasonably assumed that constant or near-constant drift conditions will prevail over the extent of a single mission. Therefore drift speed and heading were modeled as either constant or as having a constant (low) rate of change, selecting randomly between the two conditions for each state on a per-mission basis. Buoy EKF speed and heading were initialized at zero.

AUV speed measurements for EKF updates are modeled using a normal distribution with a standard deviation of 0.05 m/s. Heading measurements were taken using a compass bias modeled such that for each possible heading a bias term was added to the true value. The bias terms varied randomly between ±1º, being generated on a per-simulation basis. Ship East, North, speed and heading measurements, and buoy East and North measurements (buoy speed and heading were not measured) did not use a noise model. Those measurements are quantized and broadcast to the sub in an 8-bit payload and the quantization resolution is greater than the accuracy of the measuring instruments for each state.

In order to simulate the type of acoustic ranging errors seen in practice, range noise and random message loss were introduced in all communications. The ranging error was randomly distributed among four possible cases, based on previous experience at UI [20]. 50% of ranges were slightly longer and 35% were slightly shorter than the true range (varying up to 0.2 m in both cases), modeling small variations in sound speed and water conditions between message transmission and receipt. A further 5% of ranges were 5-10 m long, modeling potential wave reflection errors. The final 10% of messages were dropped entirely, modeling miscellaneous message loss errors and the WHOI modem's capability to detect and reject bit-transmission errors.

2) Simulation Scenarios

Three different scenarios were simulated to serve as points of comparison for the field tests. The first used standard MSBL navigation, as described in [9]. The second was HBL configuration one, which utilized the buoy EKF to track a buoy drifting randomly according to the simulation parameters detailed above. This represents a compromise between minimizing system complexity and improving localization accuracy (relative to MSBL). The system uses an additional transponder over standard MSBL, requires an additional EKF, and in practice would require additional hardware costs. In exchange it keeps the level of accuracy seen in standard MSBL and augments it with ranging data from the floating buoy for a theoretical gain in AUV localization accuracy early after initialization and throughout the remainder of the mission.

The third simulation scenario, HBL configuration two, attempts to maintain a level of system complexity similar to MSBL by offsetting the addition of the buoy transponder by removing one of the ship-mounted transponders. The theoretical gain for this system is an improvement in the rate at which the initialization error is corrected, while still receiving consistent parallel- and perpendicular-to-path range data from the ship and the buoy throughout the mission. The loss of one transponder between HBL configurations one and two is expected to reduce the AUVs' navigational accuracy, but the transponder geometry should still yield improved navigation when compared to MSBL. This scenario represents a comparable cost and minimal increase in complexity compared to MSBL.

D. *Optimization*

To maximize the usefulness of the floating buoy and improve the AUVs' EKF accuracy, optimization was performed on each of three areas: the communication cycle, the EKF coefficients (see [16]), and the buoy initial position relative to the AUV-ship waypoint path. Each area of optimization used the Monte Carlo method; optimization cost functions and parameters were derived from repeatable, random sets of simulated missions. In each case, the accuracy of the AUV EKF in a measurement zone extending 25 m ahead of and 75 m behind the location of the ship's (simulated) GPS measurement point was used as the cost function.

First optimized was the communication cycle, selecting between the two options presented above. As discussed, the selection primarily consisted of weighing the relative importance of buoy/ship EKF updates and AUV EKF range updates from the buoy.

Optimized second were the EKF coefficients used to track the buoy and AUV states. A constrained nonlinear optimization routine (MATLAB®'s '`fmincon`' function) was utilized to run an active-set constrained optimization. Initial points used for the AUV EKF were the MSBL-optimized coefficients described in [11] and the buoy EKF optimization was initialized using the ship EKF coefficients from the same source. Because the operation and update schedule for the ship EKF did not change significantly between MSBL and HBL mission configurations, ship EKF coefficients remained unchanged.

Finally, the buoy's initial position relative to the AUV-ship waypoint path was optimized. It was allowed to drift as described in the *Simulation Parameters* section, and located at 10 m intervals in a grid bounded by the waypoint path's ends in the east-west direction, and the waypoint path and boundary of the quantization zone in the north-south direction.

E. *Field Testing*

Field tests were conducted to validate the simulation results, following the configurations discussed in the *Simulation Scenarios* section.

The AUVs used for these tests have been previously developed by researchers at UI. They utilize same the MOOS path-following algorithm [19] as their simulated counterparts, and are equipped with a variety of onboard sensors. Included among these are: a capacitive pressure sensor used to calculate depth, accurate to ±0.15 m; a magnetoresistive compass with a heading accuracy of ±0.15º; and an IMU which measures acceleration along and angular velocity about three Cartesian axes. Additional information about UI's AUVs can be found in [21].

The test facility is located at the Acoustic Research Detachment of the Naval Surface Warfare Center, on Lake Pend Oreille in Idaho, with tests being performed at a barge anchored in the lake. An objective ship (seen in Fig. 4) with differential global positioning system (DGPS) capability is utilized with mounted MSBL transponders as in [9]. The ship's pilot visually navigates the waypoint path using a GPS display, and is typically accurate to with ±1.5 m of the path.

Fig. 4. The objective ship used during field testing. The MSBL transponders are attached to outriggers mounted on the sides of the ship, one of which is seen here raised to prepare for docking.

The facility is equipped with an array of fixed, bottom-mounted LBL transponders capable of receiving tracking pings from fleet AUVs and using the time difference of arrival (TDOA) method to localize the AUVs throughout the mission [22]. These tracking points are treated as an independent measurement of AUV location and are used in post-processing to determine the accuracy of navigation and localization.

The drifting buoy for HBL configurations one and two consisted of a GPS-capable transponder suspended 3 m deep from the test barge. Although this buoy setup is not freely drifting, the barge's anchored position constraint is loose enough that the AUV is still required to track its position using the onboard buoy EKF.

Based on the results of the previously described optimization process on the communication cycle, it was determined that the two potential cycles had negligibly different impacts on AUV performance. Therefore the cycle selected for all simulation and field testing of HBL navigation was the "HBL Long" cycle (see Table 1) due to the practical benefits of having a cycle evenly divisible into one minute.

III. Results

A. Simulation

The buoy location optimization results demonstrate a clear region in which the buoy is most effective. As seen in Fig. 5, the AUV EKF position error is lowest when the buoy is initialized approximately 20-70 m off the waypoint path and located west (towards the AUV starting position) of the AUV-ship crossover point by 10-40 m. This result was used to design the location of the buoy and the waypoint courses for the objective ship and AUV for both simulation and field testing.

The top half of Fig. 6 shows a representative sample run of each simulated scenario. The left column shows a top view of the true and estimated trajectories of both the objective ship and the AUV, while the right column shows the absolute position error (EKF estimate vs. true position) as a function of

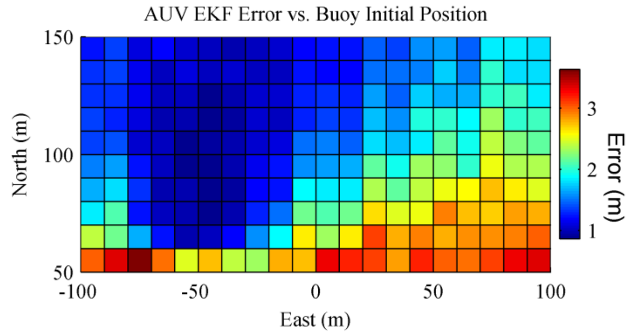

Fig. 5. Optimization results for buoy initial position relative to AUV-ship waypoint path. In this simulation, the waypoint path endpoints are at (-100, 50) and (100, 50). The AUV (traveling east) and ship (traveling west) cross at approximately -20 m East.

distance past the objective ship (negative values indicate that the ship and AUV are still heading towards each other, crossing at zero). The top half of Table 4 gives a comparison of mean tracking error for each scenario, starting with MSBL in the top row and followed below by HBL scenarios one and two. A 500-trial Monte Carlo simulation was used to calculate the mean tracking error of each of the three presented portable AUV navigation methods. As expected, the HBL configurations outperformed MSBL in simulation, with MSBL simulations having a mean tracking error of ~3.0 m and HBL simulations having a mean tracking error of ~1.4 m.

B. Field Testing

All field test results reported are taken from post-processed data which re-evaluate the AUV EKF performance using ship DGPS position (instead of EKF position) and the independent LBL tracking location of the buoy. The results of the field tests are shown on the bottom half of Fig. 6. Also shown are the results from previous MSBL field testing. The mean tracking error of each mission configuration over all field test runs is shown in the bottom half of Table 4. Five runs of HBL configuration one and three runs of HBL configuration two were performed, while 24 previous MSBL tests are also reported. The runs shown in Fig. 6 are characteristic of these field tests.

TABLE 4. Collected Mean Error Data

Evaluation Method	Configuration	Mean Tracking Error (m)
Simulation	MSBL	3.03
	HBL 1	1.37
	HBL 2	1.35
Field	MSBL	3.30
	HBL 1	1.86
	HBL 2	2.09

The mean tracking errors from field testing, shown in Table 4, follow the same pattern seen in simulation, albeit with slightly larger magnitudes. The MSBL mean tracking error for field testing was ~3.3 m vs. ~3.0 m from simulation. The mean tracking errors from field testing of HBL configurations one and two were ~1.9 m and ~2.1 m, respectively, while the values from simulation were ~1.4 m for both.

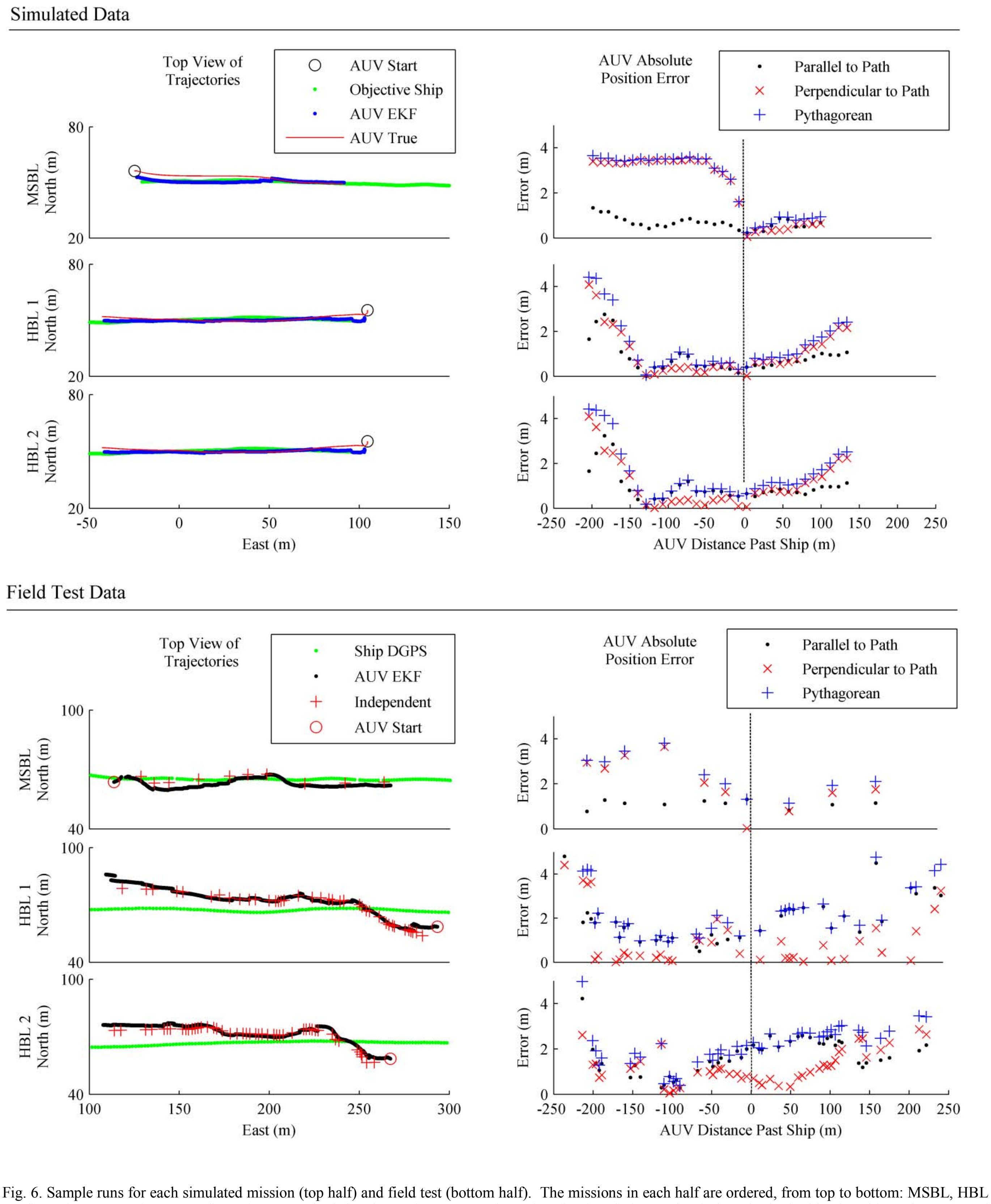

Fig. 6. Sample runs for each simulated mission (top half) and field test (bottom half). The missions in each half are ordered, from top to bottom: MSBL, HBL configuration one, and HBL configuration two. The left column shows a top view of navigation during each mission (for both objective ship and AUV), and the right column shows the absolute EKF position error relative to the AUV's distance past the objective ship (negative x-axis location indicates the AUV and ship have not yet crossed). The EKF error in simulation is compared to the simulated AUV's true position in five-second intervals, while the EKF error in field tests are compared to the points from the independent LBL tracking system.

The field testing results in Fig. 6 also show significant deviation from the desired waypoint path in both HBL configurations, especially in comparison to simulation. Although some of this is indicative of normal field testing, a significant portion of the navigational difficulty in these tests can be traced to the use of GPS rather than DGPS when measuring the buoy's location. GPS is less accurate than DGPS and can have varying accuracy when overshadowed by local structures (such conditions prevailed during testing).

IV. Discussion and Conclusions

The simulation used in this research was successful as a tool with which to evaluate the relative accuracy of different navigational approaches. In both the simulation and field test results, the mean tracking accuracy changed by a similar amount between MSBL and HBL navigation. There was minor disagreement in the magnitude of the tracking error between live and simulated tests however, indicating that the simulation could be further improved to more accurately model the physical system.

In both simulation and field testing, the HBL configurations demonstrated improved navigational accuracy over MSBL. This indicates that the addition of ranges from the floating buoy was successful in resolving some of the difficulties found in MSBL navigation.

It is further significant that the HBL two configuration, which used only a single ship-mounted transponder (in addition to the floating buoy), did not show a significant reduction in navigational accuracy over HBL configuration one. This suggests that a single parallel-to-path range source and a single perpendicular-to-path range source may be used to accurately localize an AUV. The small difference in tracking error between the two HBL methods provides freedom in selecting the one more suited to a desired task; HBL configuration one may slightly improve accuracy, but HBL configuration two is less intensive from a cost and construction standpoint.

The results of the field tests in particular show that areas exist for future improvement of this research. The comparatively poor navigational accuracy of the AUV will likely be improved by utilizing a DGPS system for buoy position measurements rather than GPS. A better approximation of ocean conditions might also be achieved by constructing a fully free-floating buoy, eliminating the artificial constraint on buoy motion caused by mounting it on an anchored barge. Finally, more field testing is necessary to expand the database of results and gain a more statistically certain picture of HBL navigation.

Acknowledgment

The authors of this paper would like to acknowledge the gracious support of the Office of Naval Research, through "Magnetic Signature Assessment System using Multiple Autonomous Underwater Vehicles (AUVs) Phase 3", ONR N00014-10-1-0883.

V. References

[1] US Department of Defense, "Unmanned system roadmap 2007-2032," 2007.

[2] R. Diamant, W. Seah, M. Waldemeyer H. Tan, "A survey of techniques and challenges in underwater localization," *Ocean Engineering*, vol. 38, no. 14-15, pp. 1663-1676, 2011.

[3] N.H. Kussat, C.D. Chadwell, and R. Zimmerman, "Absolute positioning of an autonomous underwater vehicle using GPS and acoustic measurements," *IEEE Journal of Oceanic Engineering*, vol. 30, no. 1, pp. 153-164, 2005.

[4] J. Farrel, Y. Zhao, V. Djapic P.A. Miller, "Autonomous underwater vehicle navigation," San Diego, California, 2008.

[5] D. Kronen S. Smith, "Experimental results of an inexpensive short baseline acoustic positioning system for AUV navigation," in *MTS/IEEE OCEANS Conference and Exhibition*, Halifax, Nova Scotia, 1997.

[6] P. Oliveira, C. Silvestre M. Morgado, "Tightly coupled ultrashort baseline and inertial navigation system for underwater vehicles: An experimental validation," *Journal of Field Robotics*, vol. 30, no. 1, pp. 142-170, 2013.

[7] J. Leonard P. Newman, "Pure range-only sub-sea SLAM," in *IEEE International Conference on Robotics and Automation*, 2003.

[8] B. Jouvencel, V. Creuze P. Baccou, "Single beacon acoustic for AUV navigation," in *International Conference on Advanced Robotics*, Budapest, Hungary, 2001.

[9] M. Anderson, J. Canning, D. Edwards, J. Frenzel, D. Odell, T. Bean, J. Stringfield, J. Feusi, B. Armstrong, A. Folk, B. Crosbie E. Wolbrecht, "Field testing of moving short-baseline navigation for autonomous underwater vehicles using synchronized acoustic messaging," *Journal of Field Robotics*, vol. 30, no. 4, pp. 519-535, July 2013.

[10] B. Armstrong, E. Wolbrecht, Håvard Fjær Grip A. Folk, "Autonomous underwater vehicle navigation using moving baseline on a target ship," in *IEEE Oceans '10*, Seattle, WA, 2010.

[11] J. Stringfield, Navigation andlocalization of an autonomous underwater vehicle fleet for magnetic field measurements, 2012.

[12] J.J. Leonard, J.A. Curcio, J.S. Willcox J. Vaganay, "Experimental validation of the moving long base-line navigation concept," in *IEEE/OES Autonomous Underwater Vehicles*, 2004.

[13] D. Goldberg, J. Vaganay, J. Curcio S. Willcox, "Multi-vehicle cooperative navigation and autonomy with the bluefin CADRE system," in *International Federation of Automatic Control Conference*, 2006.

[14] J. Leonard, J. Vaganay, A. Patrikalakis, A. Bahr, D. Battle, H. Schmidt, M Grund J. Curcio, "Experiments in moving baseline navigation using autonomous surface craft," in *IEEE Oceans*, 2005.

[15] E. Wolbrecht, B. Gill, M. Anderson, D. Edwards J. Feusi, "Comparison of independently-moving transponder configurations for AUV fleet navigation with one-way acoustic ranging," in *IEEE Oceans*, vol. 1, Hampton Road, VA, 2012, pp. 14-19.

[16] D. Simon, *Optimal State Estimation: Kalman, H∞, and Non-Linear Approaches*. Hoboken, NJ: Wiley-Interscience, 2006.

[17] E. Wolbrecht, D. Edwards B. Armstrong, "AUV navigation in

the presence of a magnetic disturbance with an extended Kalman filter," in *Proceedings of the MTS/IEEE OCEANS Conference and Exhibition*, Sydney, Australia, 2010.

[18] J. Partan, P. Koski, L. Freitag M. Grund, "Synchronous navigation with the micro-modem," WHOI, Tech. Rep., document Revision: D 2005.

[19] P.M. Newman, "MOOS - A mission oriented operating suite," Massachusetts Institute of Technology, Tech Rep. OE2003-07, 2003.

[20] M. Anderson, D. Edwards, M. O'Rourke, T. Bean, J. Pentzer, D. Odell J. Canning, "A low bandwidth acoustic communication strategy for supporting collaborative behaviors in a fleet of autonomous underwater vehicles," *US Navy Journal of Underwater Acoustics*, vol. 59, no. 3, pp. 285-299, 2009.

[21] et al. B. Armstrong, "Field measurement of surface ship magnetic signature using multiple AUVs," in *Proceedings of the MTS/IEEE OCEANS Conference and Exhibition*, Biloxi, MS, 2009.

[22] J. Pentzer, J. Canning, D. Edwards D. Odell, "A versatile tracking system for AUV testing," in *Proceedings of the MTS/IEEE OCEANS Conference and Exhibition*, Sydney, Australia, 2010.